

FULL-WAVE MODELING OF THE PLANCK SPACE TELESCOPE

Erik Jørgensen⁽¹⁾, Per Heighwood Nielsen⁽¹⁾, Oscar Borries⁽¹⁾, Peter Meincke⁽¹⁾

⁽¹⁾ TICRA, Laederstraede 34, 1201 Copenhagen, (Denmark),
Email: {ej,phn,ob,pme}@ticra.com

ABSTRACT

Modeling the optical system on the Planck Space Telescope pre-launch was a very demanding task, with the huge electrical size, the strict accuracy requirements and the complicated feed arrangement all posing complications for efficient modeling.

Pre-launch, the only viable option was to use a combination of physical optics (PO/PTD) for the main beam and ray optics (GO/UTD) for the sidelobes and as a coarse estimate of the effects of the structure surrounding the dual-reflector system.

Recent work, in part during an ARTES 5.2 contract with ESA, has allowed the development of a very efficient full-wave solver based on the Multi-Level Fast Multipole Method combined with a Higher-Order discretization on discontinuous meshes. In the present work, we demonstrate how this allows full-wave analysis of the LFI instrumentation of the Planck Space Telescope to be completed in a matter of hours on modest computing resources.

However, while the efficient solver allows us to find the induced surface current density on the structure with moderate computing time, other developments were necessary to allow adequately sampled full-sphere evaluation of the radiated far field.

In summary, this algorithm provides an accurate and efficient full-wave solution of structures that until recently would force engineers to use asymptotic methods.

Keywords: RF-performance, mm-Wave, Satellite, MULTI-GTD, MLFMM

1. INTRODUCTION

The flight RF performance of the PLANCK telescope was mainly based on RF calculations of the predicted in-flight geometry of the Planck satellite, cf. Figure 1. These calculations were performed using the Physical Optics method, PO, and a dedicated GTD ray-tracing algorithm, MULTI-GTD, in the GRASP program [3]. Especially the evaluation of the stray-light from the baffle and the mirrors' spill-over lobes in the 4π full sphere pattern were impossible to perform at the high frequencies between 30 GHz and 857 GHz

without using GTD due to the complex geometry and the huge electrical size of the satellite.

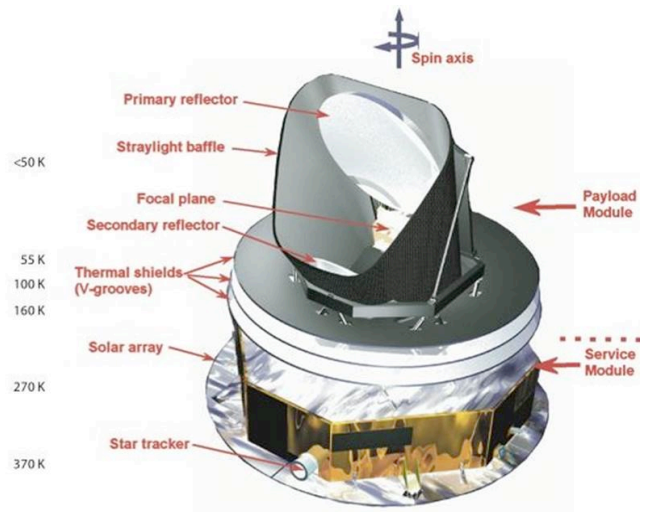


Figure 1 – Planck satellite geometry

The performed RF calculation was tested by comparing to measurements in the compact range in Cannes for a special set of the LFI detectors up to 320 GHz and using a Qualification Model of the satellite, RFQM. The agreement down to the measurement field accuracy was excellent, but some unexpected differences were found in the baffle opening direction. Using the new full-wave solution, described in Section 3, it is now possible to identify these ray contributions at 30 GHz and incorporate these in future RF simulations with higher frequencies.

The GTD/PO calculation at 30 GHz is briefly presented together with the measurements and the MLFMM results in Sections 2 and a more detailed description of the MLFMM algorithm is presented in Section 3.

2. RF PERFORMANCE AT 30 GHz

The GTD ray tracing for one stray-light direction only in the required 4π full sphere pattern is shown in Figure 2. It is a demanding task to find all the possible combination of reflections and diffractions on all the scattering structures. For that purpose a manual forward ray tracing is applied, i.e. possible ray paths are determined from the source to all the full-sphere field directions. The scatterers blocking the

rays are identified and a new ray tracing is performed, adding the reflection and the diffraction in these found scatterers. The chain is stopped when the scattered field level is insignificant compared with other field contributions. All field calculations are performed using backward ray tracing from the field direction [4].

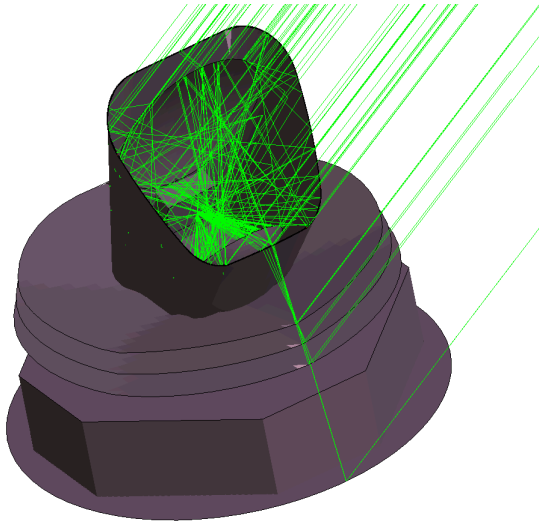


Figure 2 - RF stray light analysed by the uniform geometric theory of diffraction (GTD) method using Multi-GTD

Possible GTD caustics are detected in the field pattern of each ray contribution by searching for power spikes. If present, a UTD/PO calculation is performed and the obtained field in this pattern region is replaced. The resulting full-sphere pattern is shown in Figure 3.

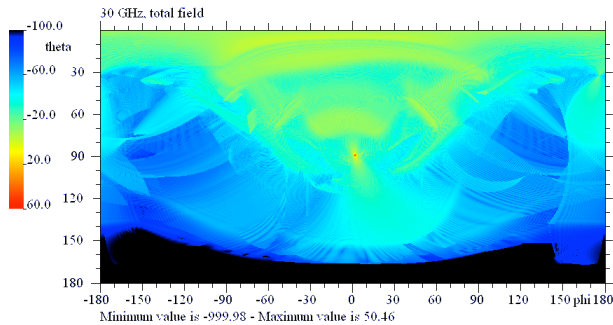


Figure 3 - Total field in $\varphi\theta$ -grid from LFI horn 28 at 30 GHz.

The $\theta = 0^\circ$ direction is in the satellite spin axis, the $\theta = 180^\circ$ direction is towards the sun and the main beam is in the $\varphi = 0^\circ$ and $\theta = 90^\circ$ directions. Up to 7 scatterers and 261 ray trace combinations have been used in this GTD calculation. The calculated performance is compared with the CPTR

measurement in the spill-over region of the 4π sphere in Figure 4.

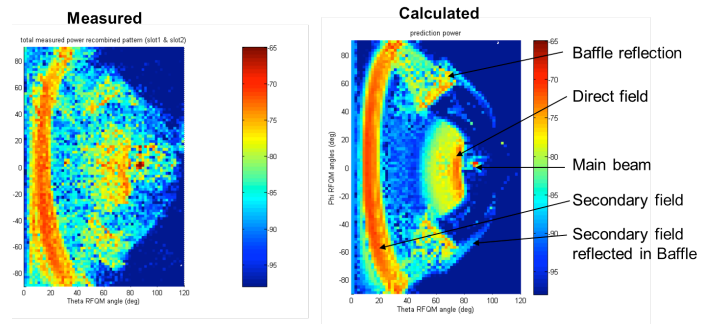


Figure 4 - CATR measurement / Numerical PO/GTD model display from max -65 dB down to max -100 dB, 30 GHz

The main stray-light lobes are seen to be very similar. Only in the baffle opening direction, $\varphi=[-30^\circ, 30^\circ]$ and $\theta=[30^\circ, 50^\circ]$, the measured field is larger than the simulated field. Applying the new MLFMM algorithm it is now possible to recalculate the performance at 30 GHz using a CAD model of the Planck satellite directly. The resulting RF performance is in the symmetry cut compared with UTD/PO field, cf. Figure 5.

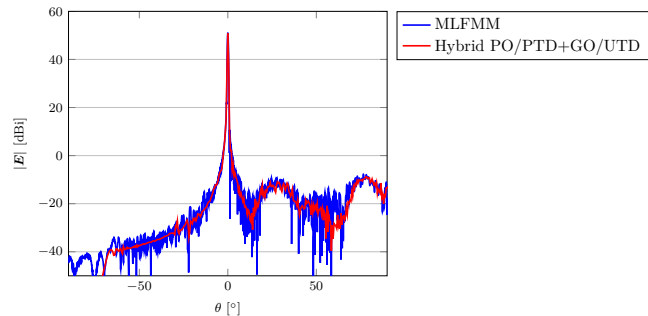


Figure 5 – Comparison between the achieved full-wave (MLFMM) solution and the original Hybrid solution used during the design of the system.

Visually, the MLFMM solution is very similar to the UTD/PO results, but near $\theta=50^\circ$ the MLFMM field is up to 10 dB larger. This field direction corresponds to the $\theta=40^\circ$ angle in the theta-phi grid pattern in figure 4 and explain the missing simulated field contribution compared to the measured pattern. By picturing of the generated currents on the Planck structures, see Figure 6, the missing GTD contribution can be detected by inspection.

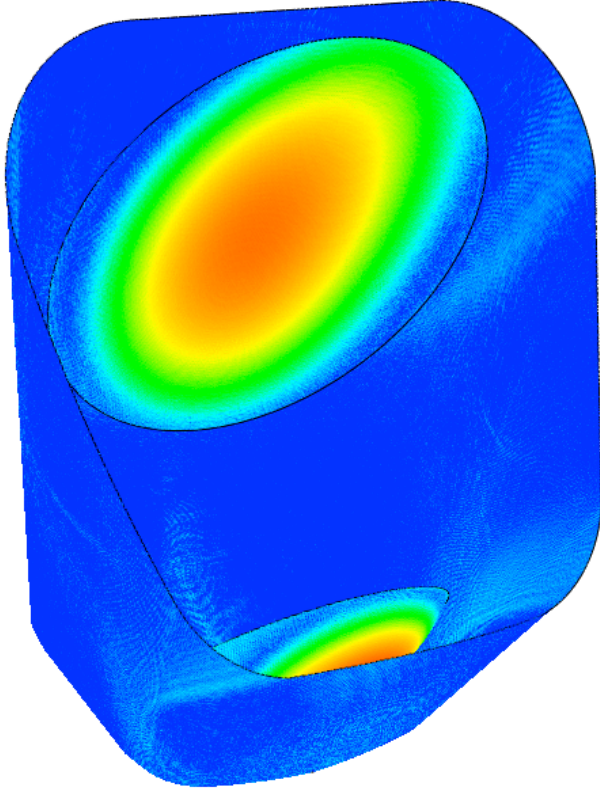


Figure 6 – Induced surface current density on the main part of the Planck Space Telescope: Baffle and reflector system

Clearly, the bottom part of the baffle is illuminated severely by the detector. This part of the satellite has not been considered in previous simulations, partly due to lacking knowledge of the exact geometry and partly due to presuming a thermal coverage film producing diffuse scattering.

3. MLFMM ALGORITHM

In this section, we describe the algorithm behind the results in Figs. 5-6.

Fundamentally, Multi-level Fast Multipole Method (MLFMM) reduces both the time and memory complexity of the Method of Moments (MoM) solution from N^2 to $N \log N$, where N is the number of unknowns. This is done by a hierarchical subdivision of the process involved in a matrix-vector product with the MoM matrix, similar to how the Fast Fourier Transform (FFT) accelerates the Discrete Fourier Transform.

While the MLFMM reduces the complexity of the solution process, it unfortunately also precludes a direct solution of

the linear MoM system of equations, requiring instead the use of an iterative solver. This means that the use of MLFMM requires that several other components, such as an iterative solver (e.g. GMRES) and a preconditioner (e.g. diagonal preconditioner), be implemented.

Furthermore, the algorithm used for the present work is MLFMM adapted to the very efficient Higher-Order (HO) basis functions used in the MoM implementation in GRASP. While the efficient combination of MLFMM and HO basis functions is not trivial, [1] discusses how such a combination allows for much faster solutions with lower memory requirements when compared to e.g. an MLFMM code based on the industry-standard Rao-Wilton-Glisson (RWG) basis functions.

The solution algorithm is thus somewhat more involved, but the reduction in memory and computation time is significant. Below is shown a table with the key computational characteristics of the problem when solved on a workstation with 2 x Intel Xeon E5-2690 and 160 GB RAM.

MLFMM Solution details for PLANCK at 30 GHz	
Electrical size	168,477 λ^2
HO unknowns	5,337,075
Equiv. RWG unknowns	$\approx 25,000,000$
Iterations	101
Memory	51 GB
Solution time	2:22 hours

Considering that a MLFMM solution based on RWG basis functions would require an estimated 0.5 TB, it is clear how the HO-MLFMM implementation provides a gigantic reduction in memory, allowing us to find the currents on the PLANCK model even while using a moderate workstation.

4. CURRENT INTEGRATION

While the currents themselves allow several interesting conclusions, as discussed in Section 3 and illustrated in Figure 6, they are not the target characteristic of the simulation.

Rather, the full sphere radiated field with adequate sampling is required, which results in another problem: The complexity of finding the radiated field from the MLFMM currents is also N^2 . Thus, while the MLFMM algorithm significantly reduces the necessary time and memory for finding the induced surface current density, the following computation of the radiated far-field from that current density becomes a bottleneck in the solution process, requiring 8.5 days.

Further, we compute the field scattered by the structure back in the focal plane. To simplify the model, we have not included all the detector geometries in the simulation, and thus this near field allows us to gauge the energy reflected back into the detectors, illustrating whether the removal of the detectors from the simulation has a significant impact on the result. Computing this near field around the focal plane of the system requires roughly 1:23 hours.

Based on these insights, an accelerated current integration algorithm was implemented in GRASP, alongside the new MLFMM implementation.

The accelerated algorithm is based on the technique discussed in [5], but with a range of improvements to allow sufficient accuracy to be achieved as discussed in [6]. Due to the high directivity of the PLANCK system, more than 100 dB of dynamic range is required to find an accurate rendition of the full sphere far-field.

A comparison between the computation times for the accelerated and direct current integration algorithms, requiring 100 dB dynamic range, is shown in the table below.

	Output points	Direct integration	Accelerated algorithm
Full-sphere	85.5 x 10⁶	8.5 days	14:29 mins
Focal plane	0.25 x 10⁶	1:23 hours	26 seconds

As the table clearly shows, the savings are extreme, allowing the full simulation process to be completed in an efficient and timely manner and removing the field computation bottleneck.

5. CONCLUSIONS

Using the new MLFMM algorithm, along with the accelerated current integration algorithm, it is now possible to calculate the exact scattered field from very electrical large structures such as Planck, even on moderate computing platforms.

With this method it has been demonstrated that missing GTD ray contributions can be identified and the old 4π full-sphere patterns can be corrected for the higher frequencies.

The algorithms that make this possible are included in GRASP 10.4 and are implemented in a way that requires no user intervention, instead using automated rules to determine when MLFMM and/or accelerated current integration is worthwhile.

REFERENCES

1. Oscar Borries et al., “Multi-Level Fast Multipole Method for Higher-Order Discretizations,” IEEE Transactions on Antennas and Propagation 62, no. 9 (September 2014).
2. Jan Tauber et al., “Planck pre-launch status: the Optical system”, Astronomy and Astrophysics 520, no. 2 (September 2010).
3. Knud Pontoppidan, GRASP manual, www.ticra.com .
4. Per Nielsen, “TICRA-Reports on the correlation of RFQM measurements to model, S-1496-01 (2009).
5. Amir Boag, “A Fast Physical Optics (FPO) Algorithm for High Frequency Scattering,” IEEE Transactions on Antennas and Propagation 52, no. 1 (January 2004).
6. Oscar Borries et al., “Analysis of Electrically Large Antennas using Fast Physical Optics,” European Conference on Antennas and Propagation, Apr. 2015, Lisbon.